State Estimation Based on Kalman Filtering Techniques in Navigation

L. Tamás[1], Gh. Lazea[1], R. Robotin[1], C. Marcu[1], S. Herle Z. Szekely[2]
Automation Department, Technical University of Cluj-Napoca, Romania[1]
{levente.tamas, gheorghe.lazea, radu.robotin, cosmin.marcu, sorin.herle}@aut.utcluj.ro
Purdue University, USA, szekelyz1@calumet.purdue.edu[2]

Abstract- **This paper tackles the problem of the position measurement and estimation techniques in the robot navigation field based on Kalman filters. It presents the problem of the position estimation based on odometric, infrared and ultrasonic measurements. Further on deals with the theoretical and practical aspects of the state estimation based on Kalman filtering techniques. From the wide range of derivatives of the Kalman filtering technique there are detailed the Extended Kalman filter and the one based on Unscented Transformation. In the second part of the paper is concluded with the results of the comparison between the different filtering algorithms and the further perspectives regarding this subject**.

Keywords- **Odometric, ultrasonic, infrared measurement, Kalman filter, unscented transformation.**

I. Introduction

The robot localization problem represents a key aspect in making a robot system a real autonomous one. It is essential for the robot to know where it is in order to determine what the is next step to perform. For the localization problem, the robot has access to the information from the localization sensors, the feedback about the driving action in the surrounding word. Based on this information the robot has to estimate its position as accurately as possible.

A. General Problem Presentation

The existence of the uncertainty in both the model and the sensing of the robot corrupt the localization problem. However, the uncertainty in the information can be reduced by applying an optimal filtering algorithm [1].

The Kalman Filter is a well-known estimation technique in the filed of estimation theory that combines the information of different uncertain sources in order to estimate the state of the robot. These types of filter have been successfully applied in a series of application from the field of navigation including the mission to Mars or missile tracking/guidance [1].

The Kalman filters covered in this paper are the Linear Kalman Filter (LKF) for LTI systems, the Extended Kalman Filter(EKF) which is suitable also for nonlinear systems, and the Unscented Kalman Filter (UKF) based on the Unscented transformation. The UKF can also be applied for systems with discontinuities and is directly comparable to second order Gauss filter [3]. Also in contrast with the original Gaussian noise distribution assumption for the LKF and EKF, the UKF does not rely on such restriction making it even more general.

B. Proposed Solution

The proposed solution presented in this paper deals with the state estimation problem in the field of mobile robots. There are presented some special aspects regarding this class of problems.

II. Kalman Filters

The Kalman filter [4][5] can be shortly described as an optimal recursive data processing algorithm for systems corrupted by noise.

Whenever the state of a system needs to be estimated from noisy sensor information, some kind of state estimator is employed to fuse the data from different sensors together to produce an accurate estimate of the true system state. When the system dynamics and observation models are linear, the minimum mean squared error (MMSE) estimate may be computed using the Linear *Kalman-Filter*-[5].

Although the Kalman filtering technique is not limited only to the state estimation problem having also important aspects in the parameter estimation domain [7], this paper deals only with the parameter estimation part of the problem.

A. Kalman Filter for Linear Systems

The LKF addresses the general problem of trying to estimate the state of a discrete-time controlled process represented on Figure 1 that is governed by the linear equation given by (1) and (2)

$$x_{k+1} = F\left(x_k, u_k, w_k\right) \tag{1}$$

$$y_k = H\left(x_k, v_k\right) \tag{2}$$

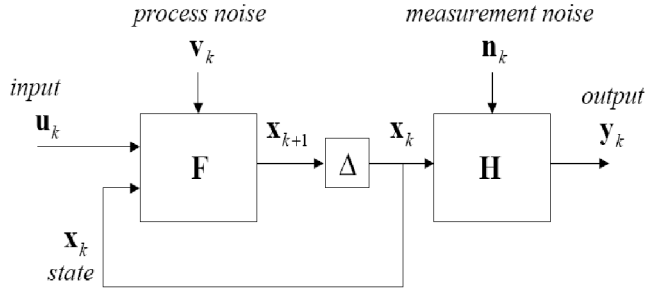

Figure 1 Discrete-time nonlinear dynamic system

The generic representation of the system in the state space is given by (3) and (4).

$$x_k = Ax_{k-1} + Bu_{k-1} + w_{k-1} \tag{3}$$

$$z_k = Hx_k + v_k \tag{4}$$

The random variables *w* and *v* represent the process and measurement noise, and it is supposed that they are white, independent noises with a Gaussian distribution and they have the covariance *R* and *Q*.

The vector *x* represents the states of the system while *z* relates the state of the measurements and *u* is the input vector for the system. The matrices *A, B, H* are assumed to be constant, although they may change from in time in real life applications.

For the further notation it is defined the "super minus" for the prior state estimate at time step *k* and his state estimate is based on the knowledge of the process prior to step *k*. The posterior state estimate is computed taken into account also the measurement information from the step *k*.

$$e_k^- \equiv x_k - \hat{x}_k^- \tag{5}$$

$$e_k \equiv x_k - \hat{x}_k \tag{6}$$

The two kinds of estimates are in fact related to the two phases of the Kalman filtering algorithm: the time update (prediction) and the measurement update (correction) [5].

The first phase of the Kalman filter can be summarized in the equations described in (7) and (8)

$$\hat{x}_k^- = A\hat{x}_{k-1} + Bu_{k-1} \tag{7}$$

$$P_k^- = AP_{k-1}A^T + Q \tag{8}$$

The *Q* represents the covariance of the process noise *v* while with *R* is denoted the covariance of the measurement noise *w*. These values also might change with time but in this algorithm, they are supposed to be constant, while P_k^- represents the estimated error covariance at time k.

After the time update step in the correction step there are updated the priory estimates.

$$K_k = P_k^- H^T \left(HP_k^- H^T + R \right)^{-1} \tag{9}$$

$$\hat{x}_k = \hat{x}_k^- + K\left(z_k - H\hat{x}_k^- \right) \tag{10}$$

$$P_k = \left(I - K_k H \right) P_k^- \tag{11}$$

The K_k matrix is called the Kalman gain and is chosen in such a way that minimizes the a posteriori error covariance P_k.

The difference in (10) is called the measurement innovation, or the residual. The residual reflects the difference between the predicted measurement and the actual measurement.

At the first step of the algorithm the values of *x* and *P* are initialized with the prior knowledge about the system. It is not a trivial task to tune the values of the covariance *R* and *Q*. These values influence the performance of the filter although there is no direct method of choosing them. In real time applications it is often the case that they are selected in a trial and error method. Details for selecting the covariance values for certain measurement types will be shown in the section describing the experimental setup.

B. Extended Kalman Filter

As it was described in the previous subsection the Kalman filter addresses the general problem of trying to estimate the state of a discrete-time controlled process that is governed by a linear stochastic difference equation.

But in reality instead of pure linear systems in the most of the cases the equations describing the systems are nonlinear. Some of the interesting and successful applications of Kalman filtering have been used for the nonlinear systems. A Kalman filter that linearizes about the current mean and covariance is referred to as an Extended Kalman filter or EKF [4].

The most common approach for the nonlinear systems is simply to linearize all nonlinearities in the models so that afterwards the linear Kalman filter can be applied. The linearization is done by computing the Jacobian of the matrices *A, B, C, D* as follows:

$$A_k \triangleq \left. \frac{\partial F\left(x, u_k, \bar{v}\right)}{\partial x} \right|_{\hat{x}_k} \qquad B_k \triangleq \left. \frac{\partial F\left(\hat{x}_k^-, u_k, v\right)}{\partial v} \right|_{\bar{v}} \tag{12}$$

$$C_k \triangleq \left. \frac{\partial H\left(x, \bar{n}\right)}{\partial x} \right|_{\hat{x}_k} \qquad \mathrm{D}_k \triangleq \left. \frac{\partial H\left(\hat{x}_k^-, n\right)}{\partial n} \right|_{\bar{n}} \tag{13}$$

Although the EKF is widely used in the control community it is difficult to implement, difficult to tune, and only stable for systems which are almost linear on the time scale of the update intervals [10].

C. Unscented Kalman Filter

Many difficulties from the *EKF* algorithm emerge from the Jacobian matrices that are calculated at the linearization phase. The *UKF* proposes a derivative free alternative for this type of filtering first being introduced by Julier et al [9][10] and further developed for state estimation and parameter estimation purposes by Merwe et al [7][11][12].

Julier and Uhlmann showed the substantial advantages of the UKF in the field of nonlinear control. The basic difference between the EKF and UKF emerges from the way that the Gaussian random variables (Grv) are propagated through the nonlinear system. While in the case of the EKF, the Grv is propagated analytically through the system by a first order linearization of the system in the case of the UKF this is performed using a deterministic sampling approach. The state distribution is also in this case represented by a Grv, but the distribution is represented by a set of sample points called *sigma points*. These sigma points capture the true mean and covariance of any nonlinear system, making the UKF directly comparable with a second order Gaussian filter. Furthermore, the nature of the filter does not require the calculation of Jacobians and the computational effort is the comparable with effort of EKF. In order to achieve this, the UKF uses the *unscented transformation.*

The unscented transformation (UT) is a method for computing the statistics of a random variable that undergoes a nonlinear transformation [10]. It is founded on the intuition that it is easier to approximate a Gaussian distribution than it is to approximate an arbitrary nonlinear function or transformation.

Although the idea of using a set of representative points in order to propagate the mean and covariance reminds the Monte-Carlo type methods[14], there is an extremely important difference: the samples (sigma points) are not drawn at random but rather according a deterministic way.

An n dimensional variable x with the mean $\bar{x}$ and with the covariance P_{xx} is approximated by a $2n+1$ weighted sigma point set as follows:

$$\begin{aligned} \mathcal{X}_0 &= \bar{x} & W_0 &= \kappa/(n+\kappa) \\ \mathcal{X}_i &= \bar{x} + \left(\sqrt{(n+\kappa)P_{xx}}\right)_i & W_i &= 1/2(n+\kappa) \\ \mathcal{X}_{i+n} &= \bar{x} - \left(\sqrt{(n+\kappa)P_{xx}}\right)_i & W_{i+n} &= 1/2(n+\kappa) \end{aligned} \quad (14)$$

where κ is scaling parameters and determines the spread of the sigma points around the mean $\bar{x}$ and $\left(\sqrt{(n+\kappa)P_{xx}}\right)_i$ denotes the i^{th} column of the matrix square root.

The transformation itself is done by propagating the selected sigma points through the nonlinear function as follows:

$$\mathcal{Y}_i = f[\mathcal{X}_i] \quad (15)$$

The mean and the covariance of the weighted product is given by (16) and (17) respectively:

$$\bar{y} = \sum_{i=0}^{2n} W_i \mathcal{Y}_i \quad (16)$$

$$P_{yy} = \sum_{i=0}^{2n} W_i [\mathcal{Y}_i - \bar{y}][\mathcal{Y}_i - \bar{y}]^T \quad (17)$$

D. An application - range reading with sonar

Although one of the common transformations in the robotic field is related to the polar-Cartesian, this represents a major problem due to the nonlinear characteristic of the transformation. The transformation is given by (18)

$$\begin{pmatrix} x \\ y \end{pmatrix} = \begin{pmatrix} r\cos\theta \\ r\sin\theta \end{pmatrix} \quad (18)$$

with

$$\nabla f = \begin{bmatrix} \cos\theta & -r\sin\theta \\ \sin\theta & r\cos\theta \end{bmatrix} \quad (19)$$

Supposing that a mobile robot detect beacons in its environment using a range-optimized sonar sensor. The sensor returns polar information (range r and bearing θ) which is converted to the Cartesian coordinates. The difficulty of the transformation arises from the physical properties of the sonar: even if the radial accuracy if fairly good, it has a rather poor bearing measurement (standard deviation in range of 15 degrees). The large bearing uncertainty causes the linearity assumption to be violated [9].

In order to show the effect of this linearization violation, there was considered on the Figure 2 the linear transformation of a measurement corrupted with Gaussian random noise. The blue plot representing the direct linear transformation based on (18) causes the measurement points to be distributed on a banana shape curve. Even worse the mean of the distribution marked with a black circle is not coinciding with the real one at (0,1).

As a solution to this kind of transformation it can be applied the UT. After applying the transformation on the same set of data, the result is according to the expected one: the mean of the transformation is coinciding with the real mean, and the covariance of the points is a circular one.

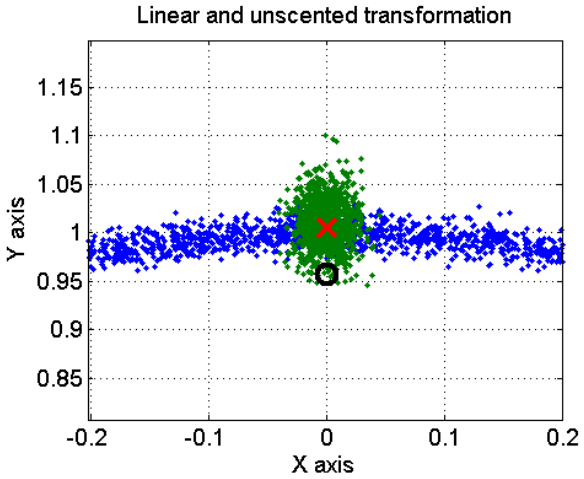

Figure 2 The linear and unscented transformation - fragment

Exploiting the advantages of the UT, the UKF algorithm at a given time instance k computes the priori estimates of the process state $\hat{x}_k^-$, its error covariance matrix P_k^- and the estimate for the output is computed using the following formulae:

$$\hat{x}_k = \sum_{i=0}^{2n} W_i^{(m)} \mathcal{X}_{i,k|k-1}^x \quad (20)$$

$$P_k = \sum_{i=0}^{2n} W_i^{(c)} \left[\mathcal{X}_{i,k|k-1}^x - \hat{x}_k^-\right]\left[\mathcal{X}_{i,k|k-1}^x - \hat{x}_k^-\right]^T \quad (21)$$

$$\mathcal{Y}_{k|k-1} = H\left[\mathcal{X}_{k|k-1}^x, \mathcal{X}_{k|k-1}^n\right] \quad (22)$$

$$\hat{y}_k = \sum_{i=0}^{2n} W_i^{(m)} \mathcal{Y}_{i,k|k-1} \quad (23)$$

The steps presented in the formulas (20), (21), (22), (23) represent the time update equations from the traditional Kalman filter. The measurement update equations are presented in the form of (24), (25), (26), (27) and (28)

$$P_{\hat{y}_k\hat{y}_k} = \sum_{i=0}^{2n} W_i^{(c)} \left[\mathcal{Y}_{i,k|k-1} - \bar{y}_k^-\right]\left[\mathcal{Y}_{i,k|k-1} - \bar{y}_k^-\right]^T \quad (24)$$

$$P_{x_k y_k} = \sum_{i=0}^{2n} W_i^{(c)} \left[\mathcal{X}_{i,k|k-1}^x - \hat{x}_k^-\right]\left[\mathcal{Y}_{i,k|k-1} - \hat{y}_k^-\right]^T \quad (25)$$

$$K_k = P_{x_k y_k} P_{y_k^- y_k^-}^{-1} \quad (26)$$

$$\hat{x}_k = \hat{x}_k + K_k\left(y_k - \hat{y}_k^-\right) \quad (27)$$

$$P_k = P_k - K_k P_{\bar{y}_k\bar{y}_k} K_k^T \quad (28)$$

As the algorithm is for the general case, it can be introduced special assumption in order to reduce from the computational effort or to enhance the performance of the filter [8].

III. MODELING

A. Dynamic Model of the System

The experiments were carried out on a P3 mobile robot platform. The coordinate system for this kind of skid-steered vehicle is presented on the Figure 3.

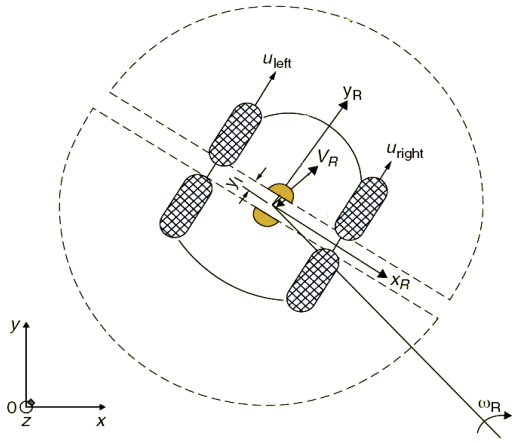

Figure 3 The coordinate system and states for the P3

The dynamic model is a terrain dependent and the parameters for the model are determined experimentally [15].

The relation between the wheel velocities on the two sides of the robot and its actual velocity in the reference coordinate system is presented in relation(29) and (30)

$$V = \begin{bmatrix} u_x & u_y & \omega_R \end{bmatrix}^T \tag{29}$$

$$V = \begin{bmatrix} a_{11} & a_{12} \\ a_{21} & a_{22} \\ a_{31} & a_{32} \end{bmatrix} \cdot \begin{bmatrix} u_R & u_L \end{bmatrix}^T \tag{30}$$

The following notations were used:

- u_x, u_y the velocity along the x and y axes with relation to the local coordinate system;
- u_R, u_L the velocity on the right/left side wheels
- ω_R the angular velocity of the robot
- a_{ij} experimentally determined coefficients

B. Odometer Positioning and Heading Estimation

The position $x_{odo,k}$, $y_{odo,k}$ and heading $\omega_{odo,k}$ at time step k are calculated using the equations (31), (32), (33), (34), (35).

$$x_{odo,k} = x_{odo,k-1} + \left(\frac{\Delta d_{R,k} + \Delta d_{L,k}}{2} \right) \cos \omega_{odo,k} \tag{31}$$

$$y_{odo,k} = y_{odo,k-1} + \left(\frac{\Delta d_{R,k} + \Delta d_{L,k}}{2} \right) \sin \omega_{odo,k} \tag{32}$$

$$\omega_{odo,k} = \omega_{odo,k-1} + \tan^{-1} \left(\frac{\Delta d_{R,k} - \Delta d_{L,k}}{W} \right) \tag{33}$$

$$\Delta d_{R,k} = d_{R,k} - d_{R,k-1} \tag{34}$$

$$\Delta d_{L,k} = d_{L,k} - d_{L,k-1} \tag{35}$$

The distances $\Delta d_{R,k}$ and $\Delta d_{L,k}$ denote the distances traveled at time step k by the right and respectively left side wheels. The W is the distance between the centers of the right and left wheels being a constant that can be measured.

C. Position and heading estimation using gyro and compass

The estimated position of the relative yaw angle of the gyroscope and the absolute yaw angle of the compass can be given by the followings:

$$x_k = t \cdot v_k \cos(\omega_k - \beta_k) + x_{k-1} \tag{36}$$

$$y_k = t \cdot v_k \sin(\omega_k - \beta_k) + y_{k-1} \tag{37}$$

The v represents the velocity of the robot along the longitudinal axes, while ω and β are the robot heading and the orientation of the body of the robot.

As the measurements with the compass in indoor conditions were rather poor quality the odometric model was adopted.

IV. EXPERIMENTAL SETUP

In the following it will be described the steps that were performed in a real life application in order to measure and estimate the position of a robot.

Both the infrared and ultrasonic measurements were carried out on a PIC microcontroller based data acquisition board. The data gather by the microcontroller were sent and processed on the PC through the serial port. The details of the experiments and the architecture of such a measurement system are described in [16].

A. Infrared Measurement

The infrared (IR) measurements were carried out by 4 pairs of emitter-receiver mounted separately in order to measure the reflection of the emitted IR signal. As a general conclusion regarding the different angle between the emitter and receiver axis it can be said that the receiver has detected the emitted signal only if it was two axes were almost on the same line.

Another aspect of the measurements is concerning the nonlinearities of the emitter-receiver pair. As it is visible on the Figure 4, there is almost a logarithmic dependency between the distance from where is reflected the IR signal and its intensity. Also the color of the object from which the signal is reflected has an important impact on the measurements.

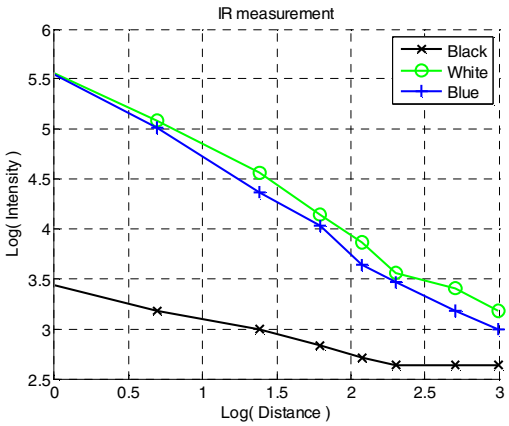

Figure 4 The IR measurement characteristics

B. Low Level Ultrasonic Measurement

The ultrasonic measurements were carried out using a pair of SR40 emitter-receiver. The received signal was sampled at 200kS/s and the distance measurement was done in a 10-200 cm range.

The main difficulty in the measurement was the detection of the first echo in a noisy measurement environment with multiple echoes.

A possible solution was proposed in [17] by computing the envelope of the received echo. A pair of emitter-receiver has a specific echo envelop for which discrete time modeling be given by (38).

$$A(kt_s) = A_0 \left(\frac{kt_s - \tau}{T} \right)^{\alpha} e^{\left(\frac{kt_s - \tau}{T} \right)} \qquad (38)$$

where the A_0 is the echo of the amplitude, α and T are specific parameters for the emitter-receiver pair; τ is the expected time of flight(TOF) and t_s is the sapling time for the measurement.

The measurement consists of the following steps:

- acquisition of the echo;
- perform a Hilbert transformation on the digital signal and take the module of the transformation in order to determine the echo of the signal
- based on the echo envelope, using parameter estimation parts of the UKF algorithm it can be determined the parameters of the (38)
- based on the determined parameters, the TOF it can be delimited with a better accuracy, or indirectly the distance of interest

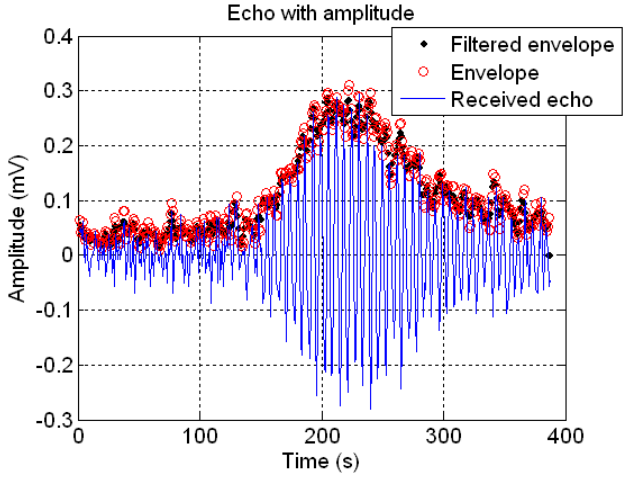

Figure 5 The echo detection with UKF – the measured signal (blue continuous), the Hilbert transformation (red envelope), estimate (black)

As it can be observed on the Figure 5 the UKF estimation of the echo envelope fits well the reference envelope. In this way it can be delimited the TOF even in the case of the high signal to noise ratio (SNR) making the measurements more accurate.

Information that can be useful for the navigation parts of the estimation is the variable accuracy of the US measurements: the absolute error of the measurement is dependent on the distance which is measured. This may help in choosing the dynamic covariance of the noise which corrupts the measurements in this case.

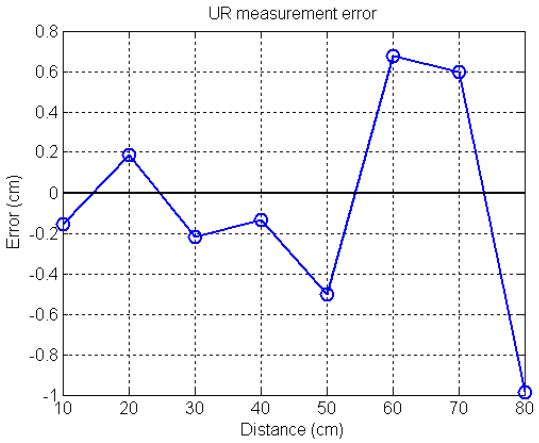

Figure 6 The absolute error variance for US measurments

C. Odometric Measurement

The odometric measurements were carried out using the dead-reckoning system of the mobile robot platform and including the inertial information [19].

As a proposed test procedure for the state estimation problem a 2X2 meter square was chosen as reference path for the mobile robot. The odometric model for the system is the one presented in (31), (32), (33).

On Figure 7 is shown the obtained measurement and the estimation of the state of the robot which has a rather noisy trajectory with certain drift in the orientation which is hard to detect even with the EKF.

During the measurement phases the position of the robot was logged continuously. Based on the reference path and the measured position vector it was computed the EKF estimate. There were tested several values for the R and Q values as they influences the results of the estimation. As it was observed, changing these values during the experiments it may have a benefic effect on the performance, for instance the covariance for the angular velocity at the corners. The covariance for the odometric measurements were chosen upon the preliminary information about the relative errors of the sensors.

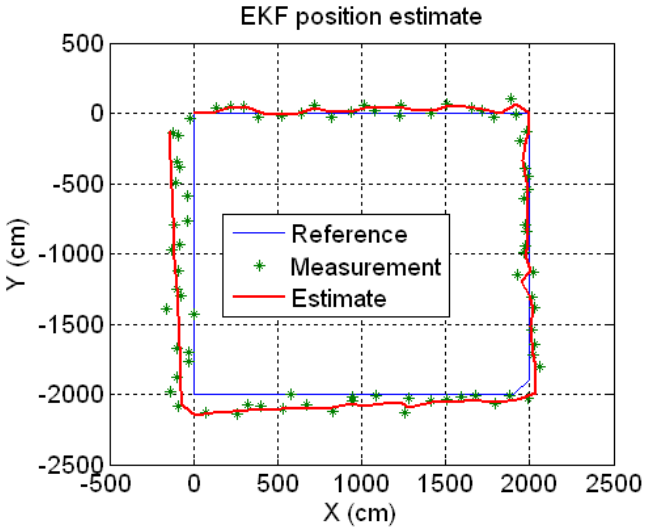

Figure 7 Odometric measurement and EKF estimation

V. Conclusions

In this paper the theoretical backgrounds of the state estimation problem was presented with real life robot applications. It can be concluded that the Kalman filter and its extensions are important tools for mobile robot state estimation. The main advantages of the different extensions of the Kalman filter can be seen in the case of the nonlinear estimations. For the nonlinear systems, several aspects have to be taken into account in applying the Kalman filter. One of the major problems was related to the computation of the Jacobian matrices. For this problem as a possible overcome it may be using UT, which eliminates the need of these computational efforts of the Jacobian matrices.

The different types of measurements are useful in case that the position estimation is not performed in a well-known medium: there may be several aspects that may corrupt these measurements.

As future proposals, the most interesting is related to the multiple data fusion aspect. According to this there are planned the state estimation to be performed based on several different types of sensors using the Kalman filter. Based on this technique it will be possible to diminish the effect of the unwanted distortions in the position estimation.

Acknowledgment

This work was supported by CNCSIS(www.cncsis.ro) project from the Romanian government and the Domus foundation(www.domus.mtaki.hu).

References

[1] R. Negenborn: Robot Locaslization and Kalman Filters, MSc. Thesis, 2003.

[2] G. Welch, G. Bishop: *An Introduction to the Kalman Filter*, UNC, 2003.

[3] S. J. Julier, J. K. Uhlmann and H. F. Durrant-Whyte. A New Approach for the Nonlinear Transformation of Means and Covariances in Linear Filters. *IEEE Transactions on Automatic Control*, 1996.

[4] P. S. Mayback, Stochastic models, estimation and control. Academic Press, Inc., New York, USA (1979).

[5] G. Welch and G. Bishop, *An Introduction to the Kalman Filter*, Chapel Hill (2001).

[6] J. Borenstein, H. Everett, Mobile robot positioning: Sensors and techniques. *Journal of Robotic Systems* 14,4 (1997).

[7] E. A. Wan and R. van de Merwe:.Dual Estimation and the Unscented Transformation. *Advances in Neural Information Processing Systems 12,* pp 666-672, MIT, 2000.

[8] R. E. Kalman: A new approach to linear filtering and prediction problems. *Trans.. ASME Journal of Basic Engineering,* pp 35-45, 1960.

[9] S.J. Julier and J. K. Uhlmann: A new approach for filtering nonlinear systems. *Proceedings of the American Control Conference, p* 1628-1632, 1995

[10] S.J. Julier and J. K. Uhlmann: A New Extension of the Kalman Filter to Nonlinear Systems. *Proc. of AeroSense: The 11th Int. Symp. on Aerospace/Defense Sensing, Simulation and Controls, 1997.*

[11] E. A. Wan and R. van de Merwe: The Unscented Kalman Filter for Nonlinear Estimation. *Proc. of Symposium 2000 on Adaptive Systems for Signal Processing, Communication and Control*, 2000, IEEE.

[12] E. A. Wan and R. van de Merwe: The square-root unscented Kalman filer for state and parameter estimation. *International Conference on Acoustics, Speech, and Signal Processing,* 2001.

[13] K. Ito and K. Xiong: Gaussian Filters for Nonlinear Filtering Problems. *IEEE Transactions on Automation Control*, 2000.

[14] V. S. Zaritskii, V. B. Svetnik: Monte-Carlo techniques in problems of optimal information processing. *Automation and Remote Conrol*, 1975

[15] K.J. Kyriakopoulos and G.C. Anousaki, "A dead-reckoning scheme for skid-steered vehicles in outdoor environments," *in Proc. Int. Conf. Robotics Automation*, May 2004, pp. 580–585

[16] Angelo M. Sabatini: A Low-Cost, Composite Sensor Array Combining Ultrasonic and Infrared Proximity Sensors *IEEE Instrumentation and Measurement Technology Conference*, pp 119-125, 1995

[17] Leopoldo Angrisani: Ultrasonic Time-of-Flight Estimation Through Unscented Kalman Filter, *IEEE Transactions On Instrumentation And Measurement*, Vol. 55, NO. 4, 2006

[18] Rasa, I: Probability Theory and Stochastic Processes*, UTPress*, 2006

[19] Lazea Gh., Tamas L., Robotin R., Marcu C.: Autonomous System For Mobile Robot Navigation, *SINTES 2007*, Craiova, Romania